Bosonic model with Z_3 fractionalization

O. I. Motrunich
Massachusetts Institute of Technology, 77 Massachusetts Ave., Cambridge, Massachusetts 02139
(Received 8 November 2002; published 17 March 2003)

A bosonic model with unfrustrated hopping and short-range repulsive interactions is constructed that realizes a Z_3 fractionalized insulator phase in two dimensions and in zero magnetic field. Such a phase is characterized as having gapped charged excitations that carry fractional electrical charge 1/3 and also gapped Z_3 vortices above the topologically ordered ground state.

DOI: 10.1103/PhysRevB.67.115108 PACS number(s): 73.43.−f, 74.25.−q

I. INTRODUCTION

A flurry of recent theoretical activity has produced specific model system realizations of fractionalized phases in two dimensions.[1–6] Essentially all of the fractionalized states constructed so far are Z_2 states.[7] On a formal level, these realizations employ the following route to Z_2 fractionalization: Strong local correlations lead to a U(1) gauge theory as a low-energy description; this gauge theory is then driven into a deconfined state by a condensation of objects carrying gauge charge 2 that also appear in the low-energy description. This formal structure has been brought out very directly in Refs. 8, 5, and 6. On a more physical level, the fractionalized insulator is produced departing from a superconducting state by a condensation of double vortices.[9,10] The main body of work concentrated on the Z_2 states since these are expected to be the simplest to realize. However, it is clear that more complicated fractionalized states are also possible. For example, it is conceivable that in some systems the superconducting state is quantum-disordered by a condensation of triple vortices; the resulting insulator is then a Z_3 fractionalized state.

In this paper, we indicate how a Z_3 fractionalized state can be engineered in a relatively simple bosonic model with unfrustrated nearest-neighbor hopping and short-range two-body repulsive interactions. Much of the construction parallels closely the Z_2 examples of Refs. 5, 6, and 3: The low-energy Hilbert space is selected—by stipulating particular charge interactions—in a manner that naturally admits splitting the boson charge into three pieces; this Hilbert space is protected by a large charge gap. The effective description of the fractionalized state has gapped chargons carrying electrical charge 1/3 and coupled to some special Z_3 gauge theory which we analyze in detail. Our main message here is that one does not need very contrived systems to obtain more complicated fractionalization patterns.

II. Z_3 VIA CHARGE FRUSTRATION

The model is defined on the lattice shown in Fig. 1, which we can think of as a hexagonal lattice with additional sites placed at the hexagon centers. We have $\psi_r^\dagger = e^{i\phi_r}$ bosons residing on the hexagonal lattice (these sites are always labeled lower case r) and $b_R^\dagger = e^{i\theta_R}$ bosons residing at the hexagon centers (uppercase R). Bosons can hop between the neighboring sites as indicated by the links on the figure; the hopping amplitudes are w_1 for $\langle r,R\rangle$ links and w_2 for $\langle r,r'\rangle$ links. We also stipulate strong repulsive interactions that favor charge neutrality of the hexagons, in addition to the on-site repulsion that favors charge neutrality of the individual sites. The complete *quantum rotor* Hamiltonian is

$$H = -w_1 \sum_{R,r\in R} (b_R^\dagger \psi_r + \text{H.c.}) - w_2 \sum_{\langle rr'\rangle} (\psi_r^\dagger \psi_{r'} + \text{H.c.}) + u_b \sum_R (n_R^b)^2 + u_\psi \sum_r (n_r^\psi)^2 + U \sum_R N_R^2 . \quad (1)$$

Here, $\{n_R^b, \theta_R\}$ are conjugate number-phase variables [e.g., in the phase representation $n_R^b \equiv -i\partial/\partial\theta_R$, $b_R^\dagger \psi_r + \text{H.c.} \equiv 2\cos(\theta_R - \phi_r)$] and similarly for $\{n_r^\psi, \phi_r\}$. The number-phase variables are particularly appropriate if we think of the model as describing an array of Josephson-coupled superconducting islands. Both b_R and ψ_r bosons carry electrical charge q_b.

In the above Hamiltonian, N_R is the boson number associated with each hexagon:

$$N_R = 3n_R^b + \sum_{r\in R} n_r^\psi . \quad (2)$$

Thus, the total boson number in the system[11] is

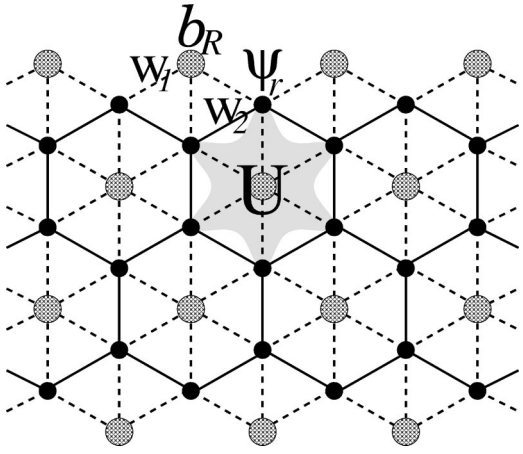

FIG. 1. Josephson junction array formed by penetrating hexagonal (r) and triangular (R) lattices, modeled by the Hamiltonian (1). The shaded area indicates schematically hexagon charging energy UN_R^2.

$$N_{\rm tot}=\frac{1}{3}\sum_R N_R. \tag{3}$$

General analysis of the possible phases proceeds as in Ref. 6. Here, we focus on the insulating states that are obtained for large $U\gg w_1,w_2,u_b,u_\psi$. If the w_1,w_2,u_b,u_ψ terms are all zero, there is a degenerate manifold of ground states specified by the requirement $N_R=0$ for each R.[12] The ground-state sector is separated by a large charge gap U from the nearest sectors. Including the w_1,w_2,u_b, and u_ψ terms lifts this degeneracy in each sector, which is best described by deriving the corresponding effective Hamiltonian in each sector.

The effective Hamiltonian in the ground-state sector ($N_R=0$) is, to third order in the perturbing terms,

$$H^{(0)}_{\rm eff}=H_{u_b,u_\psi}-J_{\rm c}\sum_r\ [(\psi^\dagger_r)^3 b_{R_1}b_{R_2}b_{R_3}+{\rm H.c.}]$$

$$-K_{\rm ring}\sum_{\hexagon}\ (\psi^\dagger_1\psi_2\psi^\dagger_3\psi_4\psi^\dagger_5\psi_6+{\rm H.c.}). \tag{4}$$

Here, H_{u_b,u_ψ} stands for the on-site repulsion terms as in Eq. (1); R_1,R_2, and R_3 label the three hexagon centers adjacent to r; $J_{\rm c}=w_1^3/(6U^2)$; and $K_{\rm ring}=3w_2^3/U^2$.

This is our main step in obtaining Z_3 fractionalization. The above Hamiltonian looks similar to a compact U(1) gauge theory coupled to a charge-3 scalar field. Thus, if we think of the ψ_r as some gauge fields, then it is very suggestive to think of the b_R as carrying gauge charge 3 [see also Eq. (2)]. Standard Fradkin-Shenker analysis[13] then suggests that by condensing the b_R field, which can be arranged by making $J_{\rm c}$ and $K_{\rm ring}$ large, we can deconfine objects carrying gauge charge 1. By virtue of Eq. (3), such objects carry fractional electrical charge $q_b/3$, and we obtain a Z_3 fractionalized insulator.

The reader who finds the above statements believable may now declare victory in achieving Z_3 fractionalization. However, if we want to describe the deconfined phase(s) in any detail, we need to study the above Hamiltonian directly since it is not related in any simple manner to conventional gauge theory. This is our focus in the remainder of the paper. Of course, we will confirm the deconfinement, but we will also find that the deconfined state that obtains for large $K_{\rm ring}$ on all hexagons is in fact a $Z_3\times Z_3$ state (see below for details).

Proceeding with this analysis, consider the regime of large $J_{\rm c}\to\infty$ and small $u_b\to 0$. It is convenient to perform the following change of variables. Define the operators $b^\dagger_{cR}=e^{i\theta_{cR}}$ and $\tilde\psi^\dagger_r=e^{i\tilde\phi_r}$:

$$b^\dagger_{cR}=s_R e^{i\theta_R/3},\quad \tilde\psi^\dagger_r=\psi^\dagger_r b_{cR_1}b_{cR_2}b_{cR_3}. \tag{5}$$

Here, $s_R=1$, $e^{i2\pi/3}$, or $e^{i4\pi/3}$, so that $\theta_{cR}\in[0,2\pi)$. One can readily verify that N_R is conjugate to θ_{cR}, while n^ψ_r is conjugate to $\tilde\phi_r$. $b^\dagger_{cR}$ carries electrical charge $q_b/3$ and can be thought of as a chargon field, while $\tilde\psi^\dagger_r$ is charge neutral. These new variables are indeed natural in the description of the deconfined phase, but to recover the physical Hilbert space, we need to impose the constraint

$$\exp\left[i\frac{2\pi}{3}\left(N_R-\sum_{r\in R}n^\psi_r\right)\right]=1. \tag{6}$$

In the new variables, the Hamiltonian becomes

$$H^{(0)}_{\rm eff}=u_\psi\sum_r\ (n^\psi_r)^2-J_{\rm c}\sum_r\ [(\tilde\psi^\dagger_r)^3+{\rm H.c.}]$$

$$-K_{\rm ring}\sum_{\hexagon}\ (\tilde\psi^\dagger_1\tilde\psi_2\tilde\psi^\dagger_3\tilde\psi_4\tilde\psi^\dagger_5\tilde\psi_6+{\rm H.c.}). \tag{7}$$

Note that we are left with gauge fields $\tilde\psi_r$ only, since we are working in the ''uncharged'' ground-state sector

The term $J_{\rm c}$ acts as a Z_3 anisotropy on the $\tilde\phi_r$ field. In the limit $J_{\rm c}\to\infty$, $e^{i\tilde\phi_r}$ becomes a Z_3 field: $\tilde\phi_r=0$, $2\pi/3$, or $4\pi/3$. The operator $P^+_r\equiv e^{-i(2\pi/3)n^\psi_r}$ shifts the states of the quantum Z_3 clock by $+1$,[14] whereas the constraints specifying the uncharged sector $N_R=0$ become

$$\prod_{r\in R}P^+_r=1. \tag{8}$$

The $u_\psi(n^\psi_r)^2$ term causes tunneling between the different states of the quantum clock, and this can be described by an effective ''transverse field'' $-h(P^+_r+P_r)$ acting on the clock.

The effective Hamiltonian now becomes Z_3 ''ring-exchange'' Hamiltonian on the hexagonal lattice of r sites:

$$-K_{\rm ring}\sum_{\hexagon}\ (\tilde\psi^\dagger_1\tilde\psi_2\tilde\psi^\dagger_3\tilde\psi_4\tilde\psi^\dagger_5\tilde\psi_6+\ {\rm H.c.})-h\sum_r\ (P^+_r+P^-_r). \tag{9}$$

The Hamiltonian together with the constraints Eq. (8) can be viewed as some special Z_3 gauge theory and is analyzed below and in further detail in Appendixes A and B. We find that generically this theory can have *two* deconfined phases (in addition to the confined phase) with the phase diagram shown in Fig. 2. Here we only describe the deconfined phase that obtains when all ring-exchange couplings are large, $K_{\rm ring}\gg h$. As explained below, this phase is a $Z_3\times Z_3$ deconfined phase.

From here on, our focus is on the above Z_3 ring-exchange Hamiltonian. We drop all tildes on Z_3 fields ψ_r and superscripts on n_r (which are now integers modulo 3). Also, we consider a Z_N generalization[14] of the above Hamiltonian and carry out the analysis in the general case. This is done for clarity of notation.

For $K_{\rm ring}\gg h$, a good caricature of the bulk ground state is given by the wave function

$$|GS\rangle=\sum_{\{n_r\}}{}'|\{n_r\}\rangle, \tag{10}$$

where the primed sum is over all configurations $\{n_r\}$ that satisfy the constraints (8), i.e., $\Sigma_{r\in R}n_r=0$.

Let us define Z_N flux through a given hexagon R,

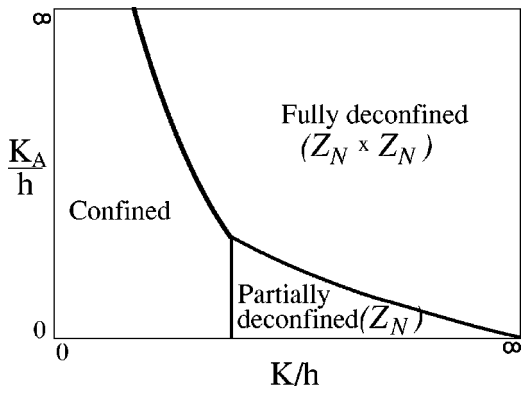

FIG. 2. Generic phase diagram of the Z_N ring exchange on hexagonal lattice, Eq. (9). To explore the different deconfined states, we allow two different ring-exchange couplings: $K_{\text{ring}}=K_A$ for *A*-type hexagons and $K_{\text{ring}}=K$ for *B*- and *C*-type hexagons (see Fig. 3).

$$\Phi_R=\phi_1-\phi_2+\phi_3-\phi_4+\phi_5-\phi_6, \tag{11}$$

with the sign convention as in Fig. 3. The ground state has zero flux through each hexagon. Excitations above this ground state are Z_N vortices. For example, we can add a unit of flux through a given hexagon by applying a ''string'' operator as indicated in Fig. 3. The gap for a vortex carrying one unit of flux is $2K_{\text{ring}}[1-\cos(2\pi/N)]$.

Observe now (Fig. 3) that the hexagon centers *R* form a triangular lattice, which consists of three sublattices *A*, *B*, and *C*. Observe also that the flux-adding string operator ''steps'' only through the same sublattice hexagons. We are thus led to the possibility of a topological distinction between vortices on the different sublattices, in addition to the

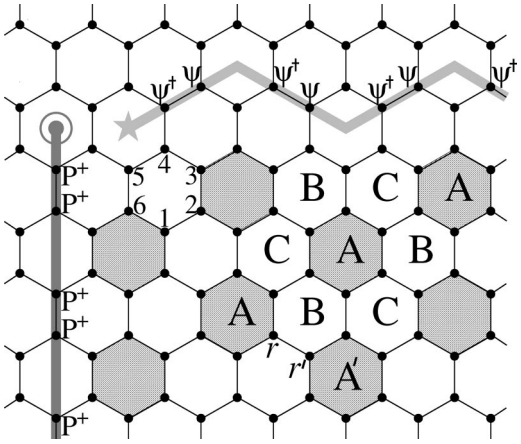

FIG. 3. Hexagonal lattice on which the Z_N ring-exchange model, Eq. (9), is defined. $N_R\equiv\Sigma_{r\in R}n_r$ measures Z_N ''number'' on each hexagon; we can increase N_R on a given hexagon ($\star$) by one by applying a ''string'' operator $\psi^\dagger\psi\psi^\dagger\psi\cdots$ along the indicated path. $\Phi_R\equiv\phi_1-\phi_2+\phi_3-\phi_4+\phi_5-\phi_6$ measures Z_N ''flux'' through a given hexagon (123456); to fix the sign convention we always take 1 to be the lowermost hexagon site. We can increase the flux through a given hexagon ($\bullet$) by one unit by applying a string $P^+P^+P^+P^+\cdots$ along the indicated path. The lower-right corner of the figure shows the three sublattice structure of the lattice of honeycombs.

TABLE I. Gauge charges of the $N_R=+1$ excitations with respect to the *A*, *B*, and *C* Z_N fluxes as defined by Eq. (11). Note that these are consistent with the fusion rules (12) and (13).

	Q_A	Q_B	Q_C
$(N_A=+1)$	0	-1	$+1$
$(N_B=+1)$	$+1$	0	-1
$(N_C=+1)$	-1	$+1$	0

usual distinction between two vortices carrying different flux. Indeed, one can see that the topologically distinct situations can be characterized by saying that we have two species of Z_N vortices, say, *A* and *B* vortices. Alternatively, if we want to preserve the symmetry among the three sublattices, we can say that there are three types of Z_N vortices—*A*, *B*, and *C* vortices—but these are not independent and instead satisfy ''fusion rules'' such as

$$(\Phi_A=+1)\times(\Phi_B=+1)\sim(\Phi_C=-1). \tag{12}$$

This means that a nearby pair of $+1$ *A* and *B* vortices is indistinguishable from a -1 *C* vortex (note also that the ''states'' on the left and on the right can be connected by local *h* terms in the Hamiltonian).

Consider now introducing Z_N charges in the above gauge theory, Eq. (9); e.g., consider placing a pair of opposite ±1 charges on two hexagons R_1 and R_2: $\Sigma_{r\in R}n_r=\delta_{RR_1}-\delta_{RR_2}$. This is appropriate when studying the charged sectors of the microscopic Hamiltonian (1) since the formal gauge structure represents the crucial coupling of chargons with the above Z_3 degrees of freedom. A charge can be added to a hexagon by applying a string operator as indicated in Fig. 3. From several perspectives, one can see that all such charges are deconfined in the $K_{\text{ring}}\gg h$ phase: Thus, in Appendix A we approach this ''fully deconfined'' phase starting from a ''partially deconfined'' phase, in which charges are deconfined on one sublattice only. Also, this fully deconfined phase corresponds to the fully disordered phase in the dual global Z_N spin model of Appendix B.

Similarly to vortices, we need to distinguish the charges on different sublattices. Again, as far as the gauge structure is concerned, we have fusion rules such as

$$(N_A=+1)\times(N_B=+1)\sim(N_C=-1). \tag{13}$$

Statistical interactions between the different particles are readily identified by studying the commutation properties of the corresponding strings. These are summarized in Table I by specifying ''gauge charges'' of the different $N_R=+1$ excitations with respect to the *A*, *B*, and *C* fluxes. Thus, $N_A=+1$ excitation carries gauge charges $Q_A=0, Q_B=-1$, and $Q_C=+1$; i.e., it does not ''see'' *A* vortices, but when transported around a *B* or *C* vortex of unit strength, the wave function acquires an additional phase $e^{-i2\pi/N}$ or $e^{i2\pi/N}$ correspondingly.

This completes the particle description of the fully deconfined phase. The minimal description would be to say that we have *A* hexagon charges that see *B* hexagon Z_N vortices and

B hexagon charges that see *A* hexagon vortices. This is essentially the claimed $Z_N \times Z_N$ structure. Thus, we expect N^2-fold ground-state degeneracy if the system is put on a cylinder, as can be verified by constructing the corresponding ground states starting from the state (10) and threading vortices through the hole of the cylinder.

It should be emphasized here that the above discussion assumed that the three-sublattice structure is respected by the boundary conditions. While it is clear that the bulk properties do not depend on this, there is an additional quirk when we consider topological degeneracy in a geometry that does not respect the three-sublattice structure. This is legitimate when all ring-exchange couplings are equal. Consider, e.g., a cylindrical geometry with the circumference along the horizontal direction of Figs. 1 and 3. When an *A*-type particle is transported around the periodic direction, it does not return to its initial position, but rather becomes a *B*- or *C*-type particle. It takes three turns for the particle to return to the original position. From Table I, such an $N_R = +1$ particle will not register any flux in this process. A detailed analysis shows that for $N \bmod 3 \neq 0$ the ground state of the system in this geometry is nondegenerate. On the other hand, for $N \bmod 3 = 0$ the ground state is found to be threefold degenerate, since in this case there is a composite object that returns to its initial state when transported once around the cylinder and that senses some flux through the hole of the cylinder in the process.

Returning to our microscopic bosonic model, the "particle description" of the $Z_3 \times Z_3$ phase is as follows: We have two species of Z_3 vortices (with gap $\sim K_{\text{ring}}$) and we have charged particles (with charge gap $\sim U$) that can be classified as carrying two distinct Z_3 gauge charges, in addition to their fractional electrical charge. Finally, note that the $Z_3 \times Z_3$ state is associated with the additional symmetries in the hexagonal lattice ring exchange Hamiltonian but is protected by the same charge gap projection, since any move within the uncharged state sector is necessarily a combination of hexagon ring exchanges.

III. CONCLUSIONS

We showed that it is possible to produce more complicated fractionalization patterns such as Z_3 fractionalization in relatively simple bosonic models. While the resulting fractionalized state turned out to be even more complicated than initially intended, the microscopic model was not too contrived. It is hoped that this work will encourage further searches for other exotic states. For example, can a non-Abelian fractionalized state be produced in a condensed matter system with a global symmetry only, short-range interactions, and in zero magnetic field?

ACKNOWLEDGMENTS

The author particularly thanks T. Senthil for many stimulating discussions and persistent encouragement that this toy project be written up and also for useful comments on the manuscript. This work was supported by the MRSEC program of the National Science Foundation under Grant Nos. DMR-9808941 and DMR-0213282.

APPENDIX A: PARTIALLY DECONFINED (Z_N) PHASE

To better appreciate the character of the deconfinement in the special gauge theory, Eq. (9), we allow different ring-exchange couplings for different hexagons and consider particular parameter space with two such couplings: $K_{\text{ring}} = K_A$ for the *A* hexagons and $K_{\text{ring}} = K_B = K_C \equiv K$ for the *B* and *C* hexagons. This is indicated schematically in Fig. 3 where the *A* hexagons are shaded. Note that by allowing the two couplings we implicitly assume that the boundary conditions on the lattice respect the three-sublattice structure; this is done throughout.

We argue below that the ring-exchange Hamiltonian has the phase diagram shown in Fig. 2 with three phases: For $h \gg K, K_A$ the system is in a fully confined phase. For $K \gg h \gg \sqrt{K_A K}$ the system is in a partially deconfined (Z_N) phase. In this phase, the charges on the *A* hexagons are deconfined, while the charges on the *B* and *C* hexagons are confined. Finally, for $K, K_A \gg h$ the system is in a fully deconfined ($Z_N \times Z_N$) phase with all charges deconfined. The phase diagram of Fig. 2 is also supported by the analysis of the dual global Z_N spin model summarized in Appendix B.

In what follows, we give a detailed description of the partially deconfined phase. As a representative of this phase, consider the Hamiltonian with $K_A = 0$, i.e., with ring exchanges around the *B* and *C* hexagons only (see Fig.3). In this case, there are additional conserved quantities

$$\hat{\mathcal{L}}_{AA'} \equiv n_r + n_{r'} = \text{const} \quad (\text{model with } K_A = 0) \qquad \text{(A1)}$$

for each hexagonal lattice link $\langle rr' \rangle$ between two *A* hexagons *A* and A' (see Fig. 3). This facilitates the analysis, since we can consider separately each subsector specified by the corresponding eigenvalues $\{\mathcal{L}_{AA'}\}$. Note that the allowed $\{\mathcal{L}_{AA'}\}$ are very much constrained by the constraints Eq. (8) on the n_r themselves; however, we will not use the details of these explicitly.

First of all, observe that the *A* hexagons in turn form a triangular lattice, while the links $\langle rr' \rangle$ between such hexagons can also be viewed as the links of this "*A* lattice," $\langle AA' \rangle \equiv \langle rr' \rangle$. In a given subsector with fixed $\{\mathcal{L}_{AA'}\}$, there remains one Z_N degree of freedom for each such link. It is convenient to work in the number basis and label these remaining link degrees of freedom by

$$\mathcal{N}_{A \to A'} \equiv n_r - n_r^{(0)} = -(n_{r'} - n_{r'}^{(0)}) \equiv -\mathcal{N}_{A' \to A}, \qquad \text{(A2)}$$

where $\{n_r^{(0)}\}$ is one particular instance: $\mathcal{L}_{AA'} = n_r^{(0)} + n_{r'}^{(0)}$ (and our convention is that $r \in A$ and $r' \in A'$—see Fig. 3). Thus, $\mathcal{N}_{AA'} \equiv \mathcal{N}_{A \to A'}$ are oriented fields on the links of the *A* lattice. The subsector is now completely specified by the conditions

$$\sum_{A' \in A} \mathcal{N}_{AA'} = 0, \qquad \text{(A3)}$$

which are the neutrality constraints Eq. (8) for the *A* hexagons.

The action of the Hamiltonian (9) in this subsector is readily described in terms of the new variables. Thus, the transverse field (h) terms are diagonal in the new number variables, while the B and C hexagon ring exchanges simultaneously raise (or lower) the three oriented number fields circulating around the corresponding A-lattice triangular plackets. Writing the raising operator for a given link number variable $\mathcal{N}_{AA'}$ as $e^{i\Xi_{AA'}}$, the resulting Hamiltonian is

$$\hat{H}[\mathcal{L}] = -K\sum_{\triangle} (e^{i\Xi_{AA'}}e^{i\Xi_{A'A''}}e^{i\Xi_{A''A}} + \text{H.c.}) - \sum_{\langle AA'\rangle} (\Gamma_{AA'}e^{-i(2\pi/N)\mathcal{N}_{AA'}} + \text{H.c.}), \quad \text{(A4)}$$

where

$$\Gamma_{AA'} = he^{-i(2\pi/N)n_r^{(0)}}(1 + e^{i(2\pi/N)\mathcal{L}_{AA'}}). \quad \text{(A5)}$$

Together with the constraints (A3), this is precisely the conventional Z_N lattice gauge theory defined on the triangular A lattice but with link-dependent $\Gamma_{AA'}$ specific for the particular subsector $\{\mathcal{L}_{AA'}\}$. We can now use the conventional wisdom to characterize each such subsector and in turn the full hexagonal ring-exchange Hamiltonian with $K_A = 0$.

When $h \equiv 0$, all the different subsectors are degenerate. The lowest-energy state in each such subsector has the energy of $-2K$ per triangle and is an equal weight superposition of all possible configurations of $\mathcal{N}_{AA'}$ that satisfy the constraints (A3). Nonzero h eliminates this degeneracy and selects one particular subsector, namely, with all $\mathcal{L}_{AA'} = 0$, as containing the true ground state of the full Hamiltonian with $K_A = 0$. Indeed, treating $\Gamma_{AA'}$ perturbatively, the lowest energy in a given subsector is

$$E_{GS}[\mathcal{L}] \approx -\sum_{\triangle} 2K - \sum_{\langle AA'\rangle} \frac{|\Gamma_{AA'}|^2}{2K[1-\cos(2\pi/N)]}, \quad \text{(A6)}$$

where for simplicity we assumed that the system has no boundaries. It is now clear that for small nonzero h the ground state of the full ring-exchange Hamiltonian with $K_A = 0$ is in the subsector with all $\mathcal{L}_{AA'} = 0$. The subsectors that are closest in energy have the smallest number of nonzero $\mathcal{L}_{AA'}$ and can be characterized as having alternating $\mathcal{L}_{A_0A'} = +1$ and $\mathcal{L}_{A_0A'} = -1$ values on the six links to a given hexagon A_0 (this subsector is obtained from the ground-state subsector by applying the hexagon ring exchange around the hexagon A_0). The energy gap to these subsectors is $6h^2/K$. We see that we have a peculiar situation where a nonzero transverse field h is needed to stabilize this Z_N deconfined ground state; this is because we are competing here against the $Z_N \times Z_N$ deconfined state that is obtained for large K_A, K.

We are all set to discuss confinement of charges in the model with $K_A = 0$. The above analysis was carried out in the uncharged sector but is readily extended to the charged sectors. First, consider placing a pair of opposite charges on two B hexagons: $\Sigma_{r\in B_1} n_r = +1$ and $\Sigma_{r\in B_2} n_r = -1$. Proceeding exactly as before, one is led to consider different subsectors (of this charged sector) specified by $\{\mathcal{L}_{AA'}\}$. In each such subsector, the Hamiltonian has precisely the form (A4) with the number variables satisfying precisely the constraints (A3). All information about the two charges is encoded in the allowed configurations $\{\mathcal{L}_{AA'}\}$, and one can clearly see that $\mathcal{L}_{AA'} \neq 0$ at least on a string of A-lattice bonds connecting B_1 and B_2. From the earlier arguments, the energy cost of introducing two such charges is then proportional to the length of this string; i.e., such charges are confined with the string tension $\sim h^2/K$.

Consider now placing a pair of opposite charges on two A hexagons A_1 and A_2: $\Sigma_{r\in A_1} n_r = +1$ and $\Sigma_{r\in A_2} n_r = -1$. The analysis of the subsectors $\{\mathcal{L}_{AA'}\}$ will be somewhat different in this case. For each such subsector in this charged sector there corresponds a subsector in the uncharged sector having exactly the same $\{\mathcal{L}_{AA'}\}$. It is convenient to "measure" each charged subsector relative to the corresponding uncharged subsector. This is achieved by defining link variables $\mathcal{N}_{AA'}$ via Eq. (A2) using an uncharged instance $\{n_r^{(0)}\}$ of $\{\mathcal{L}_{AA'}\}$ (i.e., $\Sigma_{r\in R} n_r^{(0)} = 0$ for each R and $\mathcal{L}_{AA'} = n_r^{(0)} + n_{r'}^{(0)}$ for each $\langle AA'\rangle$). In each subsector, the Hamiltonian again has the form (A4) when written in these link variables, which now satisfy new constraints $\Sigma_{A'\in A_1} \mathcal{N}_{A_1A'} = +1$ and $\Sigma_{A'\in A_2} \mathcal{N}_{A_2A'} = -1$. This corresponding precisely to introducing two charges in the corresponding A-lattice gauge theory. Clearly, for large enough $K \gg h$, these charges will be deconfined.

We now have essentially complete description of the partially deconfined phase. Thus, one can readily identify the Z_N vortex excitations of the A-lattice gauge theory with Z_N vortices on the B and C hexagons. These vortices will have usual statistical interactions with the deconfined charges on the A hexagons. Also, as should become clear by reviewing the above discussion, we can essentially account for the different subsectors $\{\mathcal{L}_{AA'}\}$ by saying that there are additional particle excitations living on the A hexagons obtained from the ground state by the action of the corresponding A-hexagon ring exchanges. These new particles have a "mass" of $6h^2/K$ and have no statistical interaction with the other particles.

We can now consider what happens when we allow nonzero K_A. As discussed above, the ring exchanges around the A hexagons introduce mixing between the different subsectors. However, as long as K_A is much smaller than the corresponding gap $\sim h^2/K$, the partially deconfined phase survives and is characterized by the same particle description.

Once K_A is sufficiently large, the system enters the fully deconfined phase described in the main text.

APPENDIX B: DUAL GLOBAL Z_N SPIN MODEL

Here we summarize dual perspective on the hexagonal-lattice ring-exchange Hamiltonian (9). We work directly in the Hamiltonian language. Simple counting shows that the dimensionality of the physical Hilbert space is consistent with having one Z_N degree of freedom per hexagon. Let us define

$$T_R^- \equiv \psi_1^\dagger \psi_2 \psi_3^\dagger \psi_4 \psi_5^\dagger \psi_6, \quad T_R^+ \equiv (T_R^-)^\dagger, \quad \text{(B1)}$$

where we use the same sign convention as in Fig. 3. Let us also define

$$V_R^\dagger \equiv \prod_{\rightarrow R} P^+, \tag{B2}$$

where the product is along the vertical path that reaches R as in Fig. 3. Note that the path ''steps'' through the same sublattice hexagons. [If we were to take some other such path, we would need to replace some P^+ with P^-. The total product is path independent due to constraints (8).] $V_R^\dagger$ can be thought of as a vortex creation operator.

We now interpret $V_R^\dagger$ as a Z_N spin variable. It is easy to verify that T_R^+ is the corresponding conjugate variable (i.e., raising operator[14]):

$$V_R^\dagger T_R^+ = e^{i2\pi/N} T_R^+ V_R^\dagger. \tag{B3}$$

Also, we can readily ''solve'' for P_r^+:

$$P_r^+ = V_{R_1}^\dagger V_{R_2}^\dagger V_{R_3}^\dagger. \tag{B4}$$

The dual Hamiltonian is

$$H = -K \sum_R (T_R^+ + \text{H.c.}) - h \sum_{\triangle} (V_{R_1}^\dagger V_{R_2}^\dagger V_{R_3}^\dagger + \text{H.c.}), \tag{B5}$$

which is a global Z_N spin model with three-spin interactions. A little thought shows that the model has in fact a $Z_N \times Z_N$ global symmetry corresponding to independent global rotations of the spins on two of the three sublattices. Note also that the three-spin interaction around triangles promotes ordering of the spins on the same sublattice. This is because two neighboring sites A and A' on the same sublattice share a BC side in the respective triangle interactions $\triangle ABC$ and $\triangle A'BC$.

The global model clearly has a fully disordered phase for $K \gg h$. In the original ring-exchange Hamiltonian, this corresponds to all vortices being gapped, and we obtain the $Z_N \times Z_N$ fully deconfined phase. Varying the A hexagon ring-exchange coupling K_A independently, for sufficiently small K_A and large K the system can clearly order on the A sublattice (i.e., A vortices condense), but remain disordered on the individual B and C sublattices. This is our partially deconfined Z_N phase.

[1] N. Read and S. Sachdev, Phys. Rev. Lett. **66**, 1773 (1991); X.-G. Wen, Phys. Rev. B **44**, 2664 (1991).

[2] R. Moessner and S. L. Sondhi, Phys. Rev. Lett. **86**, 1881 (2001).

[3] L. B. Ioffe *et al.*, Nature (London) **415**, 503 (2002).

[4] L. Balents, M. P. A. Fisher, and S. M. Girvin, Phys. Rev. B **65**, 224 412 (2002).

[5] T. Senthil and O. I. Motrunich, Phys. Rev. B **66**, 205104 (2002).

[6] O. I. Motrunich and T. Senthil, Phys. Rev. Lett. **89**, 277004 (2002).

[7] One notable example of non-Z_2 fractionalized state is the U(1) Coulomb phase in three dimensions (Ref. 6) [see also X.-G. Wen, Phys. Rev. Lett. **88**, 011 602 (2002); cond-mat/0210040 (unpublished)].

[8] S. Sachdev and M. Vojta, J. Phys. Soc. Jpn. **69**, 1 (2000).

[9] L. Balents, M. P. A. Fisher, and C. Nayak, Phys. Rev. B **60**, 1654 (1999); **61**, 6307 (2000).

[10] T. Senthil and M. P. A. Fisher, Phys. Rev. B **62**, 7850 (2000).

[11] To avoid any complications at boundaries when such are present, we require that each r site has precisely three R neighbors R_1, R_2, and R_3. We can construct such an array, e.g., by starting from a triangular lattice of the R sites, possibly with boundaries, and placing the r sites at the centers of the triangles.

[12] Recall that the operators n_R^b and $n_{rr'}^\psi$ are defined as conjugates of the corresponding phase variables and have eigenvalues that can take all integer values including negative ones; thus, the constrained Hilbert space $N_R = 0$ is indeed nontrivial.

[13] E. Fradkin and S. H. Shenker, Phys. Rev. D **19**, 3682 (1979).

[14] Each Z_N variable is represented by $\psi^\dagger = e^{i\phi} = e^{i2\pi m/N}$, $m = 0,1,\ldots,N-1$. P^+ is the raising operator on the phase ϕ and is defined by the commutation relation $e^{i\hat{\phi}} P^+ = e^{i2\pi/N} P^+ e^{i\hat{\phi}}$. It is convenient to write $P^+ = e^{-i(2\pi/N)\hat{n}}$, where n can be thought of as the number variable conjugate to the phase. Note that $\psi^\dagger$ indeed acts as a raising operator on this number as suggested by the notation.